Hindawi
Journal of Food Quality
Volume 2023, Article ID 5555608, 9 pages
https://doi.org/10.1155/2023/5555608

Research Article

Fluorescence Turns on-off-on Sensing of Ferric Ion and L-Ascorbic Acid by Carbon Quantum Dots

Ravin K. Msto,[1] **Hazha Omar Othman**,[2,3] **Baraa R. Al-Hashimi**,[4] **Diyar Salahuddin Ali**,[2,5] **Dlshad H. Hassan**,[6] **Aso Q. Hassan**,[7] **and Slim Smaoui**[8]

[1]*Collage of Pharmacy, Hawler Medical University, Erbil, Kurdistan Region, Iraq*
[2]*Chemistry Department, College of Science, Salahaddin University-Erbil, Erbil, Kurdistan Region, Iraq*
[3]*Pharmacy Department, Faculty of Pharmacy, Tishk International University, Erbil, Kurdistan Region, Iraq*
[4]*Department of Pharmacology, College of Medicine, University of Sulaimani, Sulaimani, Kurdistan Region, Iraq*
[5]*Department of Medical Laboratory Science, College of Health Sciences, Lebanese French University, Erbil, Kurdistan Region, Iraq*
[6]*Department of Biology, Faculty of Science, Soran University, Soran-Erbil, Iraq*
[7]*Department of Chemistry, College of Science, University of Sulaimani, Qliasan Street, Slemani 46002, Kurdistan Region, Iraq*
[8]*Laboratory of Microbial Biotechnology and Engineering Enzymes (LMBEE), Center of Biotechnology of Sfax (CBS), University of Sfax, Road of Sidi Mansour Km 6, P.O. Box 1177, Sfax 3018, Tunisia*

Correspondence should be addressed to Slim Smaoui; slim.smaoui@cbs.rnrt.tn

Received 1 December 2022; Revised 27 January 2023; Accepted 1 February 2023; Published 10 February 2023

Academic Editor: Sunil Pareek

This study used a hydrothermal approach to create a sensitive and focused nanoprobe. Using an "on-off-on" sensing mechanism, the nanoprobe was employed to detect and quantify ferric ions and L-ascorbic acid. Synthesis of the carbon quantum dots was achieved with a single hydrothermal step at 180°C for 24 hours using hot pepper as the starting material. The prepared CQDs showed high fluorescence with a quantum yield of 30% when excited at 350 nm, exhibiting excitation-dependent fluorescence. The emission of the CQDs can be quenched by adding ferric ions, which can be attributed to complex formation leading to nonradiative photoinduced electron transfer (PET). Adding L-ascorbic acid, which can convert ferric ions into ferrous ions, break the complex, and restore the fluorescence of CQD. The linear range and LOD were (10–90) μM and 1 μM for ferric ions, respectively, and L-ascorbic acid's linear range was (5–100) μM while LOD was 0.1 μM quantification of both substances was accomplished. In addition, orange fruit was used as an actual sample source for ascorbic acid analysis, yielding up to 99% recovery.

1. Introduction

Fluorescent carbon dots (CDs) include a large family of carbon nanomaterials, such as polymer carbon dots, graphene quantum dots, carbon nanodots, and carbon quantum dots [1]. Because of their distinctive optical characteristics, CDs have drawn significant interest in the pharmacological and biomedical analysis [2]. The compact size, excellent photoluminescence, biocompatibility, photostability, ease of preparation, and low cost of manufacture of CDs make them a promising technology [3]. Because of their unique properties, CDs are suitable for a wide range of applications, including bio(chemical) sensing [1], photocatalysis [4], thermosensing [5], light-emitting diodes [6], and cancer therapy [7].

Numerous carbon dot fabrication techniques based on both bottom-up and top-down tactics have been documented in the literature [8–10]. Bottom-up techniques involve creating carbon dots from tiny molecular or atomic precursors under high pressure and temperature [11]. Top-down techniques, on the other hand, refer to fragmenting large carbon sources into little CDs [12]. Examples of both methods are hydrothermal

[13–15], solvothermal [16], laser ablation [17], chemical oxidation [18], electrochemical oxidation [19], and arc-discharge [2], which is used commonly in carbon dot preparation.

Single-step hydrothermal method is extensively utilized in the synthesis of carbon dots. Nowadays, this method proved to be ecofriendly because it can be categorized under green chemistry, a simple, affordable, and gentle chemical approach for fabricating carbon dots. Generally, the average sizes and shapes of the CQDs are controlled by using specific precursor concentrations, processing temperatures, and reaction times [20–22].

L-ascorbic acid, referred to as vitamin C, is a necessary water-soluble vitamin found in foods like citrus fruits [23]. It is important for the human body's metabolism, growth, tissue repair, biosynthesis, and several physiological activities [24]. Through its abilities as an antioxidant that aids in scavenging free radicals and reactive oxygen species, which can have detrimental effects on human health, it has also discovered a variety of pharmaceutical applications as a supplement for the prevention or treatment of conditions like scurvy, the common cold, and cardiovascular diseases [25]. Therefore, it is crucial to determine the amount of L-ascorbic acid in pharmaceutical products accurately. As a result, numerous quantification techniques have been developed during the past few years, including high-performance liquid chromatography (HPLC) [26], colorimetry [27], capillary electrophoresis (CE) [28], titration [29], electrochemical [30], and fluorescence assays [31]. Although these techniques satisfy the need for sensitivity and precision, their main drawbacks are that they are costly, time-consuming, and require highly qualified personnel. Simple, quick, sensitive, biocompatible, and inexpensive detection techniques are necessary for the analysis of pharmaceutical components (active pharmaceutical ingredients, contaminants, and additives), and these characteristics are intrinsic to the method suggested in this study.

In this study, we developed hydrothermally produced highly fluorescent carbon quantum dots (HP-CQDs) from a naturally occurring product, hot pepper. Ferric ions were used to selectively quench the HP-CQDs, and L-ascorbic acid was used to restore them. Analytes and standard recovery percentages can both be determined using fluorometric test techniques. A concept for creating HP-CQDs with a sensing mechanism for both Fe^{3+} and L-ascorbic acid is shown in Figure 1.

2. Materials and Methods

2.1. Chemicals and Reagents. Analytical-grade chemicals and reagents were all employed in this study without further purification. Fresh hot pepper was purchased from a local store, while $Fe(NO_3)_3$, $FeCl_2$, $MnCl_2.2H_2O$, $Hg(NO_3)_2$, $CuSO_4.5H_2O$, $AlCl_3$, L-ascorbic acid, caffeine, folic acid, picric acid, and citric acid were purchased from Sigma-Aldrich. Deionized water was used for the dilution operations.

2.2. Preparation of HP-CQDs. Hot peppers were chopped and ground to prepare the HP-CQDs in a single hydrothermal process. In a 25 mL Teflon-lined stainless steel autoclave, 1 g of ground hot pepper was added along with 10 ml of deionized water. A dark brown solution was produced when the autoclave was heated to 180°C for 24 hours. The solution was then cooled to room temperature and filtered using 0.22 μm filter paper to eliminate any big undissolved particles or contaminants. The filtrate was centrifuged at 12,000 rpm for 15 minutes, followed by 20 hours of dialysis using a 1000 MWCO membrane. The finished product was preserved for further analysis and displayed blue fluorescence emission at 420 nm.

2.3. Characterization of HP-CQDs. Agilent Cary Eclipse Fluorescence Spectrophotometer (USA) was used to obtain the fluorescence spectra. At the same time, an Agilent Cary 60 Spectrophotometer (USA) was utilized to record UV-vis absorption spectra using a quartz cuvette with a path length of 1 cm. TEM images were taken using a Philips CM120 Transmission Electron Microscope (Netherlands). FTIR spectra were recorded by Perkin–Elmer Spectrum 2 FTIR Spectrometer (USA) at room temperature. The XRD pattern was obtained using a Philips PW 1730 X-ray Diffractometer (Netherlands).

2.4. Detection of the Standard of Fe^{3+}. Acetate buffer was used to keep the pH at three throughout the process, which involved mixing 1 mL of the HP-CQDs with increasing amounts of ferric nitrate solution and incubating the combination for 5 minutes at room temperature. The fluorescence intensity was next assessed in triplicate for each sample of combination.

2.5. Detection of Standard L-Ascorbic Acid. In order to bring the pH to 3, 1 mL of the HP-CQDs was combined with 1 mL of a 0.01 M ferric nitrate solution. The mixture was then incubated for 5 minutes at room temperature. The L-ascorbic acid solution was added to the mixture in escalating amounts, and the combination was incubated at room temperature for 15 minutes before the fluorescence intensity was measured.

2.6. Assay of L-Ascorbic Acid in Orange Fruit Samples. To test the suggested sensor, orange fruit was used as a sample source for ascorbic acid determination. Ascorbic acid was extracted from the material using a routine procedure that only required minor adjustments [32]. In a nutshell, the orange fruit was properly peeled, weighed, added to 50 ml of 2% oxalic acid, crushed, and centrifuged for 15 minutes at 10,000 rpm. To remove any leftover contaminants, the resultant solution was filtered through a 0.22 μm filter membrane before being stored at 5°C in a refrigerator for future analysis.

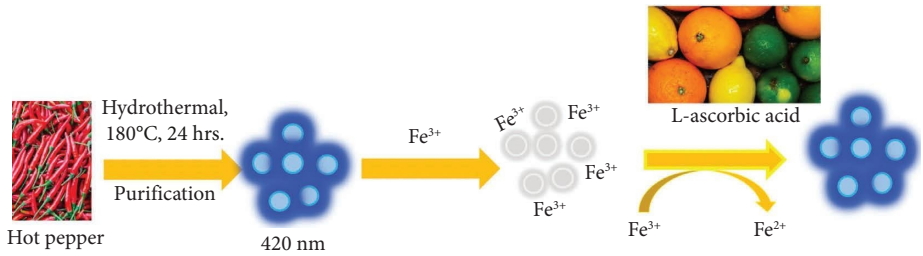

FIGURE 1: Schematic diagram of the hydrothermal preparation of the HP-CQDs, quenching by the presence of ferric ions, which is followed by fluorescence recovery by the presence of L-ascorbic acid.

3. Results and Discussion

3.1. Characterization. The TEM images (Figure 2(a)) were utilized to study the morphology of the HP-CQDs, which demonstrated that they have a diameter of around 6 nm. Moreover, the HP-CQDs were also characterized by HR-TEM, obtaining a lattice d-spacing of 0.34 nm (Figure 2(b)) which confirms that the obtained HP-CQDs are of crystalline graphitic nature [33].

The results of X-ray diffraction (XRD) shown in (Figure 2(c)) demonstrated a broad peak around $2\Theta = 23.9^{\circ}$, which can be attributed to the graphite structure of the HP-CQDs [34]. The elemental analysis of the synthesized HP-CQDs shown in Figure 2(d) gives the current weight of each element present in HP-CQDs.

Both UV-vis and fluorescence spectroscopy were used to examine the optical characteristics of the HP-CQDs. The UV-vis spectra (Figure 3(a)) showed a tiny peak at about 260 nm that results from the electrons' $\pi = \pi$ transition because C=C bonds are present [35]. Furthermore, another broad peak is observed at 345 nm that can be related to n to π^*, which originates from C=O or C–OH present on the surface of the HP-CQDs [36]. According to the fluorescence spectra (Figure 3(b)), HP-CQDs exhibit excitation-dependent emission fluorescence, and their highest emission was seen at 420 nm when excited at 350 nm (Figure 3(c)). L-ascorbic acid can be added to HP-CQDs to reverse the quenching of the fluorescence intensity brought on by the addition of ferric ions; however, the resulting complex of HP-CQDs: Fe^{3+}-L-ascorbic acid has a bathochromic effect on the emission spectra, shifting it to a longer wavelength [37] (Figure 3(d)).

The functional groups of the HP-CQDs were studied using FTIR spectroscopy (Figure 4). Two peaks are observed at 3650 and 3550 cm^{-1} which can be attributed to the presence of NH_2 groups on the surface of the carbon quantum dots. Another characteristic peak is observed at 2120 $cm^{-1,}$ which originates from either C≡C or N≡C bonds, while the bond at 1610 cm^{-1} can be designated to the C=C group.

3.2. Stability of the HP-CQDs. Under a variety of circumstances, including variable pH levels, ionic strengths, radiation levels, and temperatures, the stability of the HP-CQDs fluorescence intensity were investigated. Over the pH range of 1 to 10, the fluorescence intensity did not change much; however, a drop was seen at a strongly alkaline pH of 12 (Figure 5(a)), which can be caused by protonation and deprotonation of the surface functional groups [38]. Furthermore, when the carbon dots were dissolved in NaCl solution with an ionic strength of up to 2 M, no discernible changes in the fluorescence intensity of the carbon dots were seen (Figure 5(a)). In addition, a low reduction in fluorescence intensity was seen throughout a wide temperature range of 20 to 145°C, confirming the carbon dots' thermal resilience (Figure 5 B). The HP-CQDs were then exposed to radiation using a broad-spectrum xenon light (100 mW/cm^2), which demonstrated excellent photostability of the carbon dots even after 30 hours of radiation exposure (Figure 5(b)). The HP-CQDs' stability under extreme pH, temperature, radiation, and ionic strength increases the adaptability and reliability of the suggested analytical approach.

3.3. Determination of Fe^{3+} and L-Ascorbic Acid. Fe^{3+} ions were incrementally added to the HP-CQDs solution, and this led to a reduction in the fluorescence emission intensity (Figure 6(a)), showing high linearity in the range of 10 to 90 μM with the R^2 value being 0.9949 (Figure 6(b)) and the limit of detection being 1 μM. When L-ascorbic acid was added to the HP-CQDs: Fe^{3+} complex, the fluorescence emission intensity of the HP-CQDs increased (Figure 6(c)), showing high linearity in the range of 5 to 100 μM with the R^2 value being 0.9908 (Figure 6(d)) and the limit of detection being 0.1 μM.

3.4. Mechanism of "On-Off-On" Sensing by Fe^{+3} and L-Ascorbic Acid. To understand the theory behind the off-on phenomenon, it is imperative to study the UV-vis spectra of the HP-CQDs alone and both the HP-CQDs: Fe^{3+} and HP-CQDs: Fe^{3+}: AA (Figure 7). Because of the formation of a complex between the HP-CQDs and Fe^{3+}, which results in the ferric ions serving as an electron acceptor and causing nonradiative photoinduced electron transfer (PET), the addition of the Fe^{3+} to the HP-CQDs solution caused considerable alterations in the UV-vis spectra [39]. In addition, the addition of L-ascorbic acid caused the emission fluorescence intensity to recover due to the redox properties of L-ascorbic acid and the conversion of Fe^{3+} to Fe^{2+}, which cannot form a complex with the HP-CQDs, consequently restoring the fluorescence intensity.

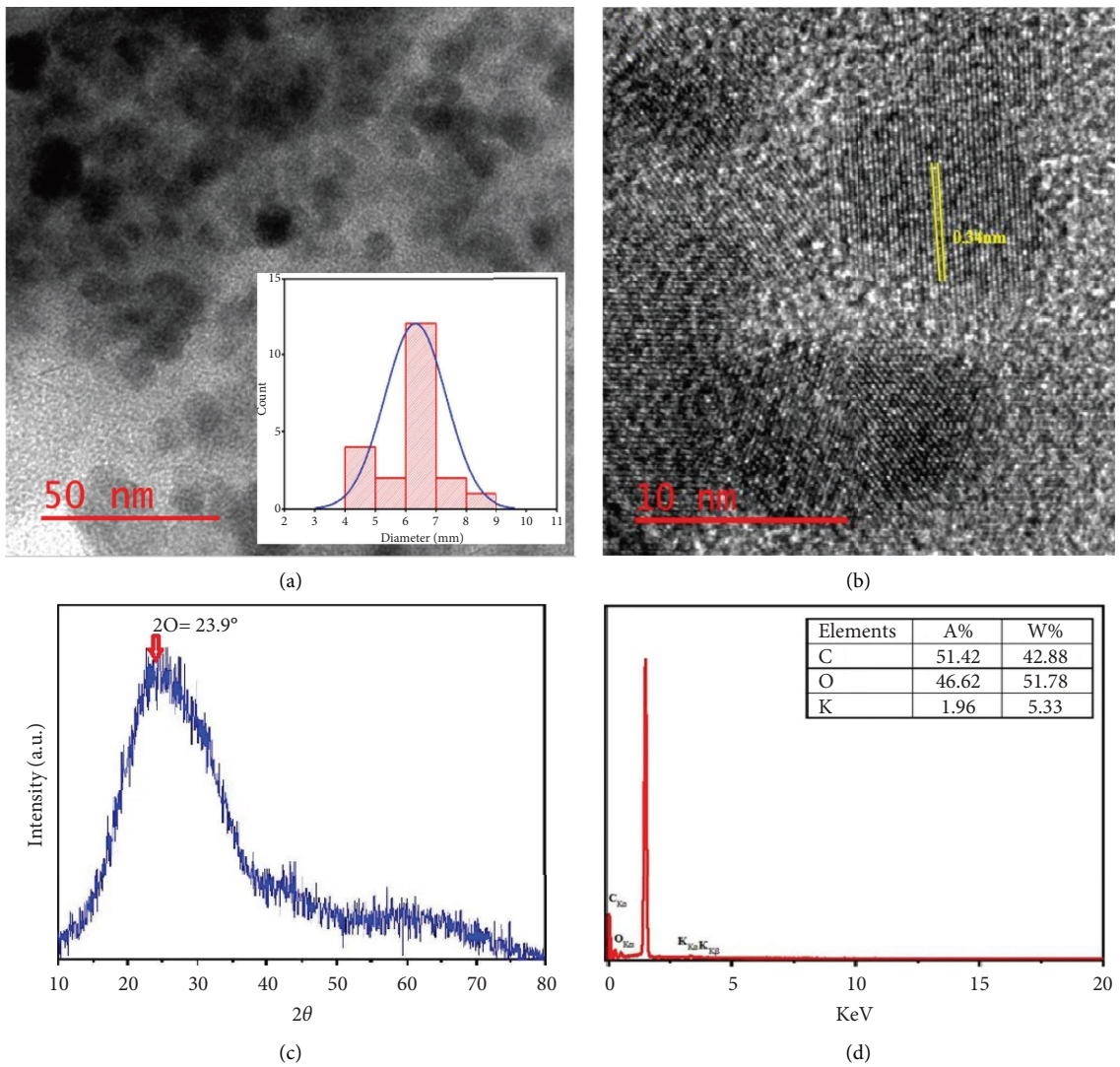

Figure 2: (a) TEM image and size distribution inset, (b) HR-TEM image and lattice spacing, (c) X-ray diffraction spectrum of the HP-CQDs, and (d) EDX analysis.

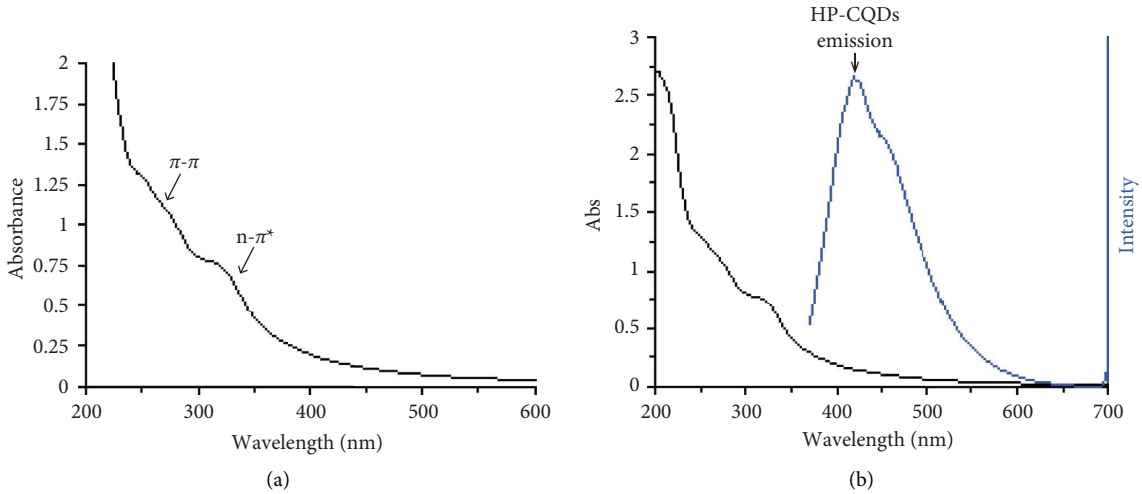

Figure 3: Continued.

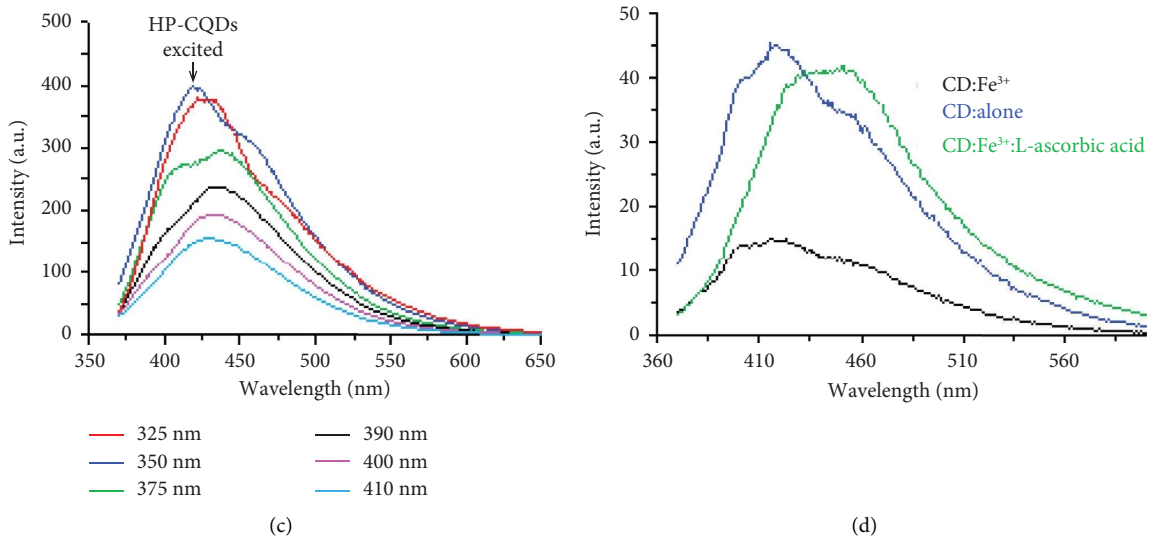

Figure 3: (a) UV-vis absorbance spectrum of HP-CQDs in the solution. (b) Absorbance and emission spectrum of HP-CQDs; the excited wavelength was 350 nm. (c) Fluorescence spectrum at different excitation wavelengths. (d) Fluorescence spectra of HP-CQDs (alone), HP-CQDs: Fe^{3+}, and HP-CQDs: Fe^{3+}-L-ascorbic acid.

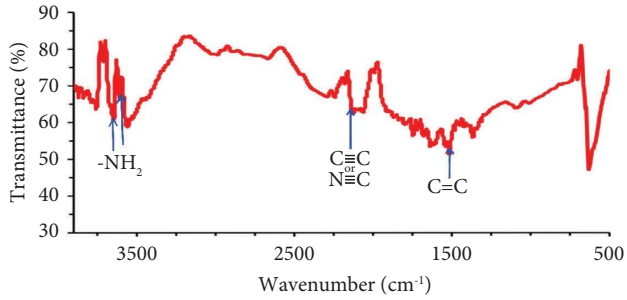

Figure 4: FTIR spectrum of the HP-CQDs.

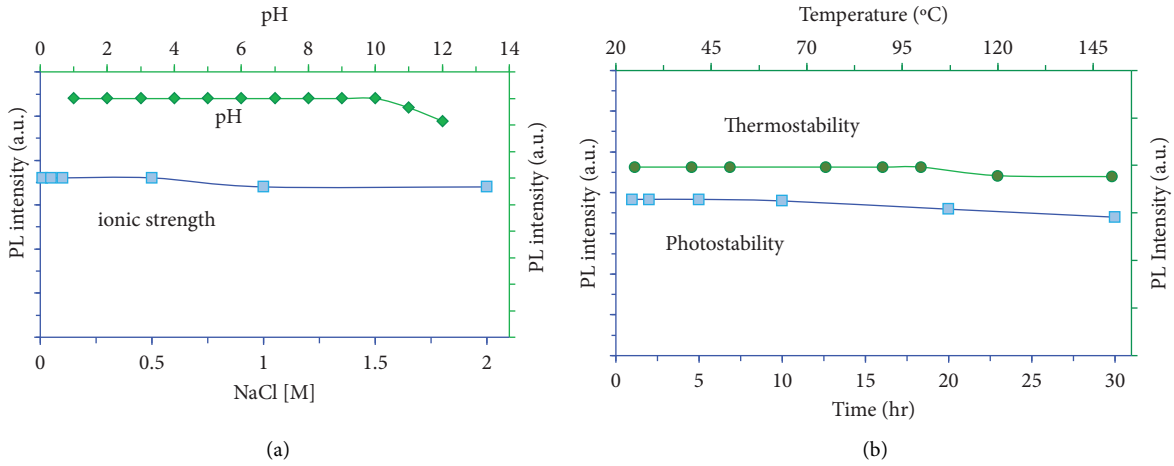

Figure 5: (a) Effects of pH and ionic strength on the intensity of HP-CQDs. (b) Effects of temperature and radiation on the intensity of HP-CQDs.

3.5. Determination of Ascorbic Acid via Restoring the Fluorescence. Ascorbic acid is simple to detect selectivity and sensitivity by observing the restored fluorescence of HP-CQDs. With increasing AA concentration, the fluorescence restoration of the HP-CQDs: Fe^{3+} system rises linearly. The relative fluorescence intensity (F/F_0) versus ascorbic acid

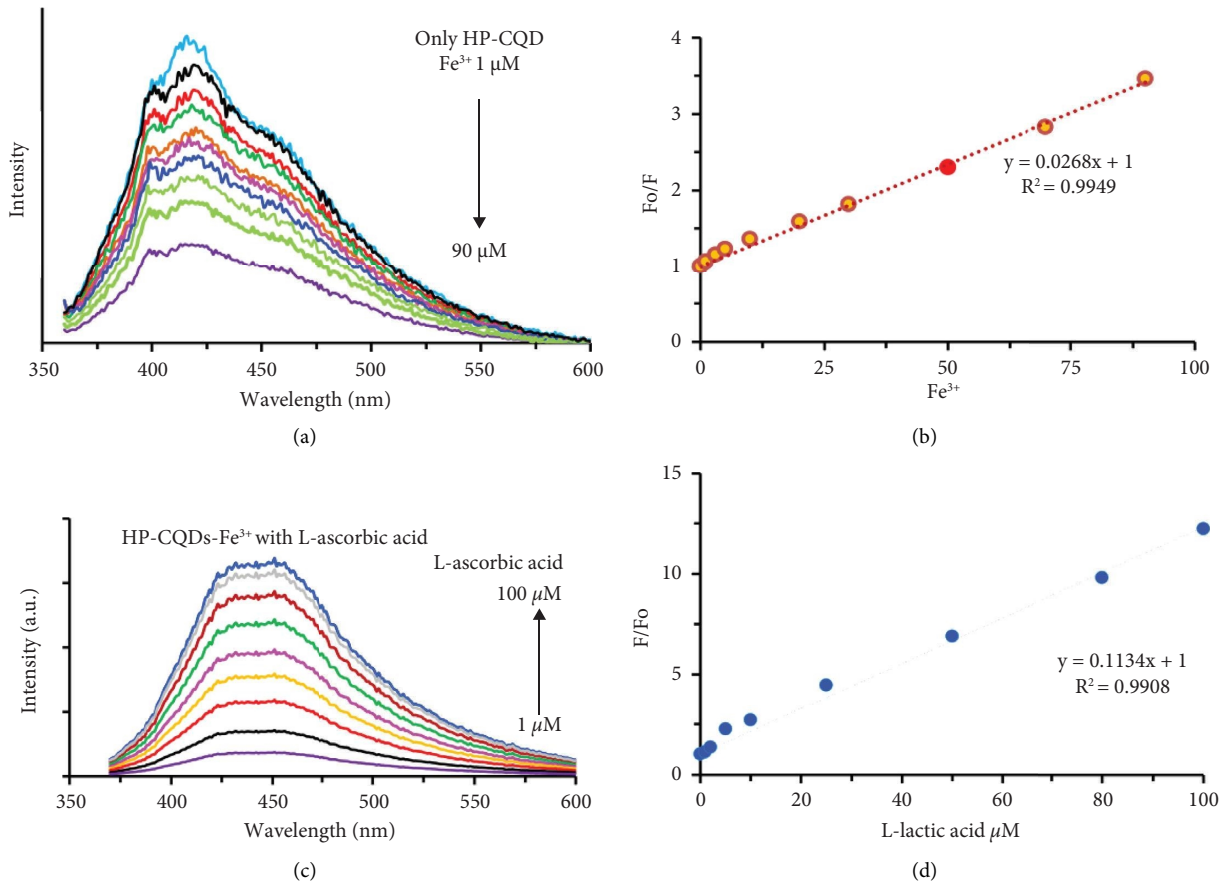

Figure 6: (a) Fluorescence spectra of serial solutions of HP-CQDs: Fe^{3+}, the fluorescence spectra were recorded when excited at 350 nm. (b) Calibration graph of HP-CQDs: Fe^{3+} solutions. (c) Fluorescence spectra of serial solutions of HP-CQDs: Fe^{3+}-L-ascorbic acid, and the fluorescence spectra were recorded when excited at 350 nm. (d) Calibration graph of HP-CQDs: Fe^{3+}-L-ascorbic acid solutions.

concentration is presented in Figure 8, where F_0 and F are the fluorescence intensities of the HP-CQDs–Fe^{3+} system in the absence and presence of ascorbic acid, respectively.

There was a 0.980 linear correlation coefficient found. The limit of detection for ascorbic acid using this technique is predicted to be 0.1 M for the proposed test. Tables 1 and 2 provide a comparison of this sensor's performance with those of other pertinent sensors.

3.6. Selectivity of HP-CQDs and HP-CQDs: Fe^{3+}. The interferences from ions other than Fe^{3+}, such as Mn^{2+}, Al^{3+}, Fe^{+2}, Hg^{2+},' and Cu^{2+}, were studied by mixing them with the HP-CQDs solution (Figure 9). This demonstrated that the addition of these metals had no effect on the fluorescence intensity and that the HP-CQDs were only selectively quenched by Fe^{3+} ions. Figure 9 shows the selectivity experiment for L-ascorbic acid detection employing a collection of biomolecules comprising urea, glucose, cysteine, glycine, and citric acid. It can be shown that only L-ascorbic acid can significantly increase PL intensity recovery, proving that the fluorescent probe that was built was extremely selective for L-ascorbic acid.

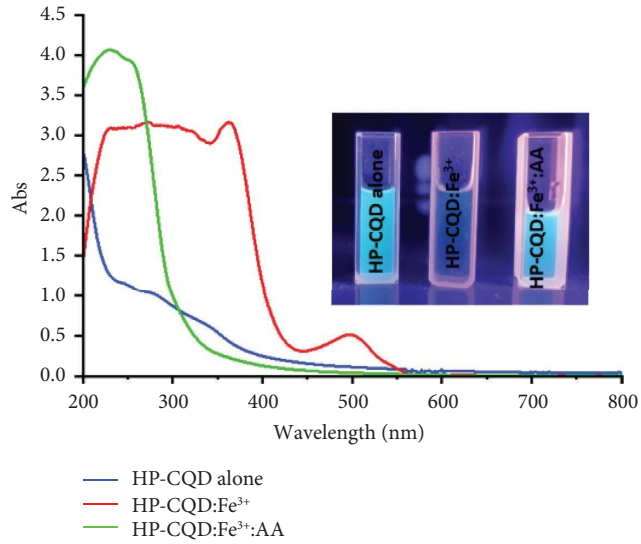

Figure 7: UV-vis spectra and inset image describe the mechanism of on-off-on of HP-CQD for sensing of Fe^{3+} and L-ascorbic acid.

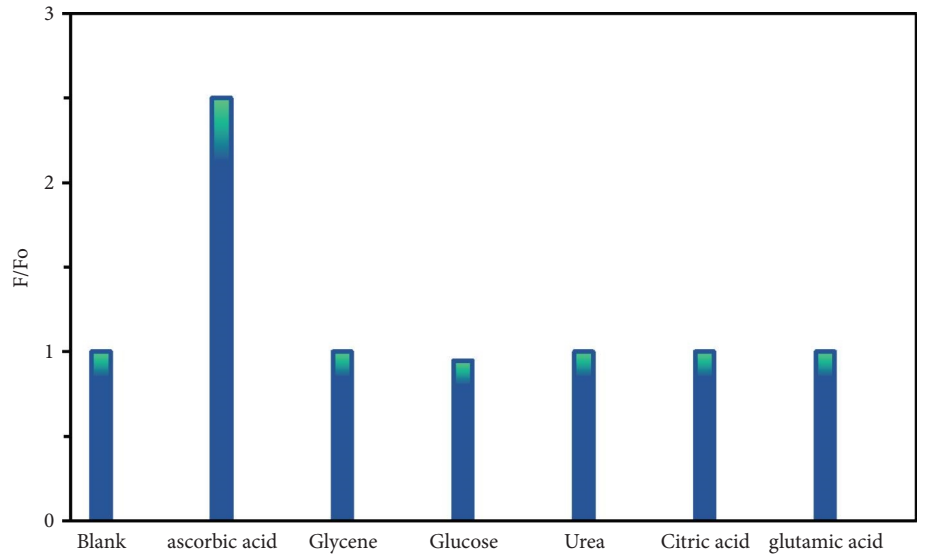

Figure 8: Selectivity of HP-CQDs for ascorbic acid.

Table 1: Comparison of different carbon dots sensors for the determination of ascorbic acid.

Precursor	Method	Sample type	LOD	Linear range	Reference
Diethylenetriamine-pentaacetic acid	Calcination	Wastewater	0.15 μM	2.5–400 μM	[40]
Citric acid and diethylenetriamine	Solvothermal	—	0.03 mmol/L	0.03–0.1 mmol/L	[31]
Citric acid and ethylenediamine	Hydrothermal	Jujube fruit	3.11 μM	5–350 μM	[41]
Citric acid and ethylenediamine	Hydrothermal	Kiwi fruit	3.17 μM	5–70 μM	[42]
Citric acid and thiourea	Hydrothermal	Fruits	4.69 μM	10–200 μM	[43]
Ascorbic acid	Microwave	—	0.05 μM	0.2–284 μM	[44]
Hot pepper	Hydrothermal	Orange fruit	0.1 μM	5–100 μM	This study

Table 2: Comparison of different carbon dots sensors for the determination of Fe^{+3}.

Precursor	Method	Sample type	LOD (μM)	Linear range	Reference
Citric acid and urea	Solvothermal	Tap water	50	0.1–0.9 μM	[16]
Garlic	Solvothermal	Tap water	0.2	0–500 μM	[45]
Hydroxymethyl aminomethane and glycerinum	Solvothermal	Lake water	50	0.05–3.1 mM	[46]
Phenylalanine and citric acid	Hydrothermal	Tap water	0.72	5.0–500.0 μM	[47]
L - glutamic acid and ethylenediamine	Microwave	Tap water	3.8	8–80 μM	[48]
Hot pepper	Hydrothermal	—	1	10–90 μM	This study

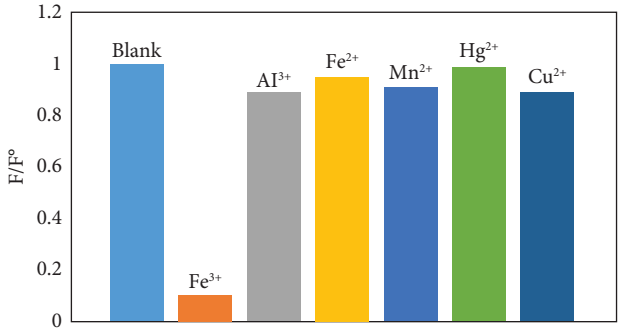

Figure 9: Selectivity of HP-CQDs and HP-CQDs: Fe^{3+}.

Table 3: Determination of ascorbic acid in the real sample.

Sample	Added (μM)	Found (μM)	Error (%)	Recovery (%)
Orange fruit	0.125	0.121	3.2	96.8
	0.310	0.298	3.8	96.0
	0.520	0.515	0.95	99.0
	0.710	0.685	3.5	96.0

3.7. Real Sample Detection in Orange Fruit. This sensor was employed to detect ascorbic acid in orange fruit to indicate the reliability of the HP-CQDs: Fe^{3+} system in ascorbic acid detection. The detection results are displayed in Table 3, in which the spiked recoveries range from 96 to 99%.

4. Conclusion

In conclusion, utilizing hot pepper as a precursor, extremely fluorescent carbon quantum dots were produced in a single step via green hydrothermal synthesis. The nonradiative photoinduced electron transfer (PET) of the HP-CQDs by the addition of ferric ions, followed by the recovery of fluorescence by the addition of L-ascorbic acid due to the conversion of Fe^{+3} to Fe^{+2}, is the proposed mechanism for the "off-on" sensing platform. Various extreme circumstances of pH, temperature, radiation, and ionic strength, which had a minor influence on the fluorescence intensity, were used to establish the stability of the carbon dots. Low detection limits of 1 M for Fe^{+3} and 0.1 M for L-ascorbic acid were achieved, while the measurement of ferric ions and L-ascorbic acid was carried out with good accuracy, precision, and recovery percentage. Finally, a real sample analysis conducted on orange fruit showed a high recovery level of 96–99%.

Data Availability

The data used to support the findings of this study are included in the article. Raw data are available from the corresponding author upon request.

Conflicts of Interest

The authors declare that they have no conflicts of interest.

Authors' Contributions

Ravin K. Msto, Dlshad H. Hassan, Hazha Omar Othman, Aso Hassan, and Diyar Salahuddin Ali were involved in investigation, conceptualization, methodology, data curation, and writing the original draft; Aso Hassan contributed to the resources analysis; Diyar Salahuddin Ali, Aso Q. Hassan, and Baraa R Al-Hashimi were involved in software and validation; and Slim Smaoui was involved in visualization, editing, validation, and supervision.

References

[1] I. Khan, K. Saeed, and I. Khan, "Nanoparticles: properties, applications and toxicities," *Arabian Journal of Chemistry*, vol. 12, no. 7, pp. 908–931, 2019.

[2] I. Singh, R. Arora, H. Dhiman, and R. Pahwa, "Carbon quantum dots: synthesis, characterization and biomedical applications," *The Turkish Journal of Pharmaceutical Sciences*, vol. 15, no. 2, pp. 219–230, 2018.

[3] S. Anwar, H. Ding, H. Bi et al., "Recent advances in synthesis, optical properties, and biomedical applications of carbon dots," *ACS Applied Bio Materials*, vol. 2, no. 6, pp. 2317–2338, 2019.

[4] H. Yu, R. Shi, Y. Zhao et al., "Smart utilization of carbon dots in semiconductor photocatalysis," *Advanced Materials*, vol. 28, no. 43, pp. 9454–9477, 2016.

[5] L. J. Mohammed and K. M. Omer, "Carbon dots as new generation materials for nanothermometer," *Nanoscale Research Letters*, vol. 15, no. 1, pp. 1–21, 2020.

[6] X. Guo, C. F. Wang, Z. Y. Yu, L. Chen, and S. Chen, "Facile access to versatile fluorescent carbon dots toward light-emitting diodes," *Chemical Communications*, vol. 48, no. 21, pp. 2692–2694, 2012.

[7] F. Wu, H. Su, Y. Cai, W. K. Wong, W. Jiang, and X. Zhu, "Porphyrin-implanted carbon nanodots for photoacoustic imaging and in vivo breast cancer ablation," *ACS Applied Bio Materials*, vol. 1, no. 1, pp. 110–117, 2018.

[8] J. Sierra-Pallares, T. Huddle, J. Garcia-Serna et al., "Understanding bottom-up continuous hydrothermal synthesis of nanoparticles using empirical measurement and computational simulation," *Nano Research*, vol. 9, no. 11, pp. 3377–3387, 2016.

[9] Y. Choi, Y. Choi, O. H. Kwon, and B. S. Kim, "Carbon dots: bottom-up syntheses, properties, and light-harvesting applications," *Chemistry--An Asian Journal*, vol. 13, no. 6, pp. 586–598, 2018.

[10] Y. Yang, D. Wu, S. Han, P. Hu, and R. Liu, "Bottom-up fabrication of photoluminescent carbon dots with uniform morphology via a soft–hard template approach," *Chemical Communications*, vol. 49, no. 43, pp. 4920–4922, 2013.

[11] S. Zhu, X. Zhao, Y. Song, S. Lu, and B. Yang, "Beyond bottom-up carbon nanodots: citric-acid derived organic molecules," *Nano Today*, vol. 11, no. 2, pp. 128–132, 2016.

[12] P. Zuo, X. Lu, Z. Sun, Y. Guo, and H. He, "A review on syntheses, properties, characterization and bioanalytical applications of fluorescent carbon dots," *Microchimica Acta*, vol. 183, no. 2, pp. 519–542, 2016.

[13] T. Ogi, K. Aishima, F. A. Permatasari, F. Iskandar, E. Tanabe, and K. Okuyama, "Kinetics of nitrogen-doped carbon dot formation via hydrothermal synthesis," *New Journal of Chemistry*, vol. 40, no. 6, pp. 5555–5561, 2016.

[14] R. Atchudan, T. N. J. I. Edison, K. R. Aseer, S. Perumal, N. Karthik, and Y. R. Lee, "Highly fluorescent nitrogen-doped carbon dots derived from Phyllanthus acidus utilized as a fluorescent probe for label-free selective detection of Fe3+ ions, live cell imaging and fluorescent ink," *Biosensors and Bioelectronics*, vol. 99, pp. 303–311, 2018.

[15] R. Atchudan, T. N. J. I. Edison, D. Chakradhar, S. Perumal, J. J. Shim, and Y. R. Lee, "Facile green synthesis of nitrogen-doped carbon dots using Chionanthus retusus fruit extract and investigation of their suitability for metal ion sensing and biological applications," *Sensors and Actuators B: Chemical*, vol. 246, pp. 497–509, 2017.

[16] K. M. Omer, D. I. Tofiq, and A. Q. Hassan, "Solvothermal synthesis of phosphorus and nitrogen doped carbon quantum dots as a fluorescent probe for iron (III)," *Microchimica Acta*, vol. 185, no. 10, pp. 466–468, 2018.

[17] S. Reyes, "Mini-mental state examination (MMSE): translation and validation for a Mexican Elderly Population. Aceptado para su publicación en Aging," *Neuropsychology and Cognition*, vol. 11, no. 1, pp. 1–11, 2004.

[18] F. Yan, Y. Jiang, X. Sun, Z. Bai, Y. Zhang, and X Zhou, "Surface modification and chemical functionalization of carbon dots: a review," *Microchimica Acta*, vol. 185, no. 9, 2018.

[19] L. Bao, Z. L. Zhang, Z. Q. Tian et al., "Electrochemical tuning of luminescent carbon nanodots: from preparation to luminescence mechanism," *Advanced Materials*, vol. 23, no. 48, pp. 5801–5806, 2011.

[20] P. Krishnaiah, R. Atchudan, S. Perumal, E. S. Salama, Y. R. Lee, and B. H. Jeon, "Utilization of waste biomass of Poa pratensis for green synthesis of n-doped carbon dots and its

application in detection of Mn2+ and Fe3+," *Chemosphere*, vol. 286, Article ID 131764, 2022.

[21] R. Atchudan, T. N. J. I. Edison, S. Perumal, N. Muthuchamy, and Y. R. Lee, "Hydrophilic nitrogen-doped carbon dots from biowaste using dwarf banana peel for environmental and biological applications," *Fuel*, vol. 275, Article ID 117821, 2020.

[22] R. Atchudan, T. N. J. I. Edison, S. Perumal, R. Vinodh, and Y. R. Lee, "Betel-derivednitrogen-doped multicolor carbon dots for environmental and biological applications," *Journal of Molecular Liquids*, vol. 296, Article ID 111817, 2019.

[23] O. Arrigoni and M. C. De Tullio, "Ascorbic acid: much more than just an antioxidant," *Biochimica et Biophysica Acta (BBA) - General Subjects*, vol. 1569, no. 1-3, pp. 1–9, 2002.

[24] A. C. Carr and S. Maggini, "Vitamin C and immune function," *Nutrients*, vol. 9, no. 11, p. 1211, 2017.

[25] D. J. Lane and D. R. Richardson, "The active role of vitamin C in mammalian iron metabolism: much more than just enhanced iron absorption!" *Free Radical Biology and Medicine*, vol. 75, pp. 69–83, 2014.

[26] V. Spínola, E. J. Llorent-Martínez, and P. C. Castilho, "Determination of vitamin C in foods: current state of method validation," *Journal of Chromatography A*, vol. 1369, pp. 2–17, 2014.

[27] W. Huang, Y. Deng, and Y. He, "Visual colorimetric sensor array for discrimination of antioxidants in serum using MnO2 nanosheets triggered multicolor chromogenic system," *Biosensors and Bioelectronics*, vol. 91, pp. 89–94, 2017.

[28] X. Qian, Q. Zhang, Y. Zhang, and Y. Tu, "Separation/determination of flavonoids and ascorbic acid in rat serum and excrement by capillary electrophoresis with electrochemical detection," *Analytical Sciences*, vol. 26, no. 5, pp. 557–560, 2010.

[29] L. Suntornsuk, W. Gritsanapun, S. Nilkamhank, and A. Paochom, "Quantitation of vitamin C content in herbal juice using direct titration," *Journal of Pharmaceutical and Biomedical Analysis*, vol. 28, no. 5, pp. 849–855, 2002.

[30] G. Maduraiveeran, M. Sasidharan, and V. Ganesan, "Electrochemical sensor and biosensor platforms based on advanced nanomaterials for biological and biomedical applications," *Biosensors and Bioelectronics*, vol. 103, pp. 113–129, 2018.

[31] L. Kong, X. Chu, W. Liu, Y. Yao, P. Zhu, and X. Ling, "Glutathione-directed synthesis of Cr (VI)-and temperature-responsive fluorescent copper nanoclusters and their applications in cellular imaging," *New Journal of Chemistry*, vol. 40, no. 5, pp. 4744–4750, 2016.

[32] H. Rao, H. Ge, Z. Lu et al., "Copper nanoclusters as an on-off-on fluorescent probe for ascorbic acid," *Microchimica Acta*, vol. 183, no. 5, pp. 1651–1657, 2016.

[33] N. Vasimalai, V. Vilas-Boas, J. Gallo et al., "Green synthesis of fluorescent carbon dots from spices for in vitro imaging and tumour cell growth inhibition," *Beilstein Journal of Nanotechnology*, vol. 9, no. 1, pp. 530–544, 2018.

[34] S. Qu, X. Wang, Q. Lu, X. Liu, and L. Wang, "A biocompatible fluorescent ink based on water-soluble luminescent carbon nanodots," *Angewandte Chemie International Edition*, vol. 51, no. 49, pp. 12215–12218, 2012.

[35] D. Bera, L. Qian, T. K. Tseng, and P. H. Holloway, "Quantum dots and their multimodal applications: a review," *Materials*, vol. 3, no. 4, pp. 2260–2345, 2010.

[36] D. Pan, J. Zhang, Z. Li, C. Wu, X. Yan, and M. Wu, "Observation of pH-solvent-spin-and excitation-dependent blue photoluminescence from carbon nanoparticles," *Chemical Communications*, vol. 46, no. 21, pp. 3681–3683, 2010.

[37] C. M. Carbonaro, R Corpino, M Salis et al., "On the emission properties of carbon dots: reviewing data and discussing models," *Chimia*, vol. 5, no. 4, p. 60, 2019.

[38] Z.-Q. Xu, L. Y. Yang, X. Y. Fan et al., "Low temperature synthesis of highly stable phosphate functionalized two color carbon nanodots and their application in cell imaging," *Carbon*, vol. 66, pp. 351–360, 2014.

[39] X. Gong, W. Lu, M. C. Paau et al., "Facile synthesis of nitrogen-doped carbon dots for Fe3+ sensing and cellular imaging," *Analytica Chimica Acta*, vol. 861, pp. 74–84, 2015.

[40] P. Li, Y. Hong, and S. F. Li, "Carbon dots-based fluorescent sensor for nanoscale sensing," *Nanoscale Imaging, Sensing, and Actuation for Biomedical Applications XVI*, vol. 10891, 2019.

[41] T. Wang, H. Luo, X. Jing, J. Yang, M. Huo, and Y. Wang, "Synthesis of fluorescent carbon dots and their application in ascorbic acid detection," *Molecules*, vol. 26, no. 5, p. 1246, 2021.

[42] T. Zhao, C. Zhu, S. Xu et al., "Fluorescent color analysis of ascorbic acid by ratiometric fluorescent paper utilizing hybrid carbon dots-silica coated quantum dots," *Dyes and Pigments*, vol. 186, Article ID 108995, 2021.

[43] X. Luo, W. Zhang, Y. Han et al., "N, S co-doped carbon dots based fluorescent "on-off-on" sensor for determination of ascorbic acid in common fruits," *Food Chemistry*, vol. 258, pp. 214–221, 2018.

[44] J. Gong, X. An, and X Yan, "A novel rapid and green synthesis of highly luminescent carbon dots with good biocompatibility for cell imaging," *Nouveau Journal de Chimie*, vol. 38, no. 4, pp. 1376–1379, 2014.

[45] C. Sun, Y. Zhang, P. Wang et al., "Synthesis of nitrogen and sulfur co-doped carbon dots from garlic for selective detection of Fe3+," *Nanoscale Research Letters*, vol. 11, no. 1, pp. 110–119, 2016.

[46] Y. Li, Y. Liu, X. Shang, D. Chao, L. Zhou, and H. Zhang, "Highly sensitive and selective detection of Fe3+ by utilizing carbon quantum dots as fluorescent probes," *Chemical Physics Letters*, vol. 705, pp. 1–6, 2018.

[47] Z.-F. Pu, Q. L. Wen, Y. J. Yang et al., "Fluorescent carbon quantum dots synthesized using phenylalanine and citric acid for selective detection of Fe3+ ions," *Spectrochimica Acta Part A: Molecular and Biomolecular Spectroscopy*, vol. 229, Article ID 117944, 2020.

[48] Y. Chen, X. Sun, W. Pan, G. Yu, and J. Wang, "Fe3+-sensitive carbon dots for detection of Fe3+ in aqueous solution and intracellular imaging of Fe3+ inside fungal cells," *Frontiers of Chemistry*, vol. 7, p. 911, 2019.